

Scientific paper

Zinc(II) Complexes Derived from Schiff Bases: Syntheses, Structures, and Biological Activity

Ling-Wei Xue,* Xu Fu, Gan-Qing Zhao and Qing-Bin Li

College of Chemistry and Chemical Engineering, Pingdingshan University, Pingdingshan Henan, 467000 P.R. China

* Corresponding author: E-mail: pdschemistry@163.com

Received: 01-06-2020

Abstract

Three new zinc(II) complexes, $[\text{Zn}_2\text{I}_2(\text{L}^1)_2]$ (**1**), $[\text{Zn}(\text{HL}^2)_2(\text{NCS})_2]$ (**2**), and $[\text{ZnIL}^3]$ (**3**), where L^1 is the anionic form of 2-[(6-methylpyridin-2-ylimino)methyl]phenol (HL^1), HL^2 is the zwitterionic form of 2-(cyclopropyliminomethyl)-5-fluorophenol (HL^2), and L^3 is the anionic form of 5-bromo-2-[(3-morpholin-4-ylpropylimino)methyl]phenol (HL^3), have been prepared and characterized by elemental analyses, IR, UV and NMR spectra, and single crystal X-ray crystallographic determination. Complex **1** is a dinuclear zinc complex, and complexes **2** and **3** are mononuclear zinc complexes. The Zn atoms in the complexes are in tetrahedral coordination. The effect of the complexes on the antimicrobial activity against *Staphylococcus aureus*, *Escherichia coli*, and *Candida albicans* were evaluated.

Keywords: Zinc complex, Schiff base, Crystal structure, Antimicrobial activity

1. Introduction

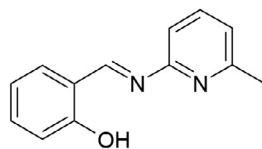
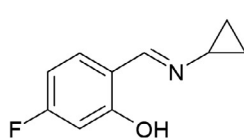
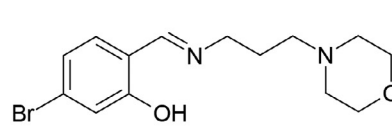
The rapid increasing interest in the synthesis and structural studies of Schiff bases is due to their bioactivity and coordination properties.¹ Schiff bases are active against fungal, cancer, convulsant, oxidant and diuretic activities.² Metal complexes of Schiff bases have attracted considerable attention due to their versatile biological activity, such as antifungal, antibacterial and antitumor.³ And, in general, the metal complexes have higher biological activities than the free Schiff bases. It has been shown that the Schiff base complexes derived from salicylaldehyde and its derivatives with primary amines, bearing the N_2O , N_2S , NO_2 or NSO donor sets, have potential antimicrobial activities.⁴ Zinc is an important biological element, its complexes derived from Schiff bases have received particular attention due to their interesting antimicrobial potential.⁵ Recent research indicated that the halide and pseudohalide groups can severely increase the antimicrobial activities.⁶ Our research group has reported some metal complexes with effective anti-

microbial activities.⁷ In pursuit of new and efficient antimicrobial agents, in the present work, three new zinc(II) complexes, $[\text{Zn}_2\text{I}_2(\text{L}^1)_2]$ (**1**), $[\text{Zn}(\text{HL}^2)_2(\text{NCS})_2]$ (**2**), and $[\text{ZnIL}^3]$ (**3**), where L^1 is the anionic form of 2-[(6-methylpyridin-2-ylimino)methyl]phenol (HL^1), HL^2 is the zwitterionic form of 2-(cyclopropyliminomethyl)-5-fluorophenol (HL^2), and L^3 is the anionic form of 5-bromo-2-[(3-morpholin-4-ylpropylimino)methyl]phenol (HL^3) (Scheme 1), are reported. To our knowledge, only two complexes with HL^1 ,⁸ and no complexes with HL^2 and

2. Experimental

2.1. Material and Methods

Salicylaldehyde, 4-fluorosalicylaldehyde, 4-bromo-salicylaldehyde, 2-amino-6-methylpyridine, cyclopropylamine, and 3-morpholin-4-ylpropylamine were purchased from Fluka. Other reagents and solvents were analytical grade and used without further purification. Ele-

HL¹HL²HL³ HL³ have been reported so far.

Scheme 1. The Schiff bases

mental (C, H, and N) analyses were made on a PerkinElmer Model 240B automatic analyser. Zinc analysis was carried out by EDTA titration. Infrared (IR) spectra were recorded on an IR-408 Shimadzu 568 spectrophotometer. UV-Vis spectra were recorded on a Lambda 900 spectrometer. X-ray diffraction was carried out on a Bruker SMART 1000 CCD area diffractometer. ^1H and ^{13}C NMR spectra were recorded on a Bruker 300 MHz spectrometer.

2. 2. Synthesis of the Ligands

2. 2. 1. 2-[(6-Methylpyridin-2-ylimino)methyl]phenol (HL¹)

Salicylaldehyde (1.22 g, 0.01 mol) and 2-amino-6-methylpyridine (1.06 g, 0.01 mol) were reacted in methanol (50 mL) for 30 min at 20 °C. The solvent was removed by distillation to give yellow product of HL¹. Analysis Calcd. (%) for C₁₃H₁₂N₂O: C 73.56, H 5.70, N 13.20. Found (%): C 73.41, H 5.82, N 13.05. IR data (KBr, cm⁻¹): 1623 (CH=N). UV in acetonitrile (λ, ε): 273 nm, 1.03 × 10⁴ L mol⁻¹ cm⁻¹; 350 nm, 2.77 × 10³ L mol⁻¹ cm⁻¹. ^1H NMR (300 MHz, *d*⁶-DMSO): δ 12.11 (s, 1H, OH), 8.63 (s, 1H, CH=N), 7.68–7.64 (m, 3H, ArH and PyH), 7.46 (t, 1H, ArH), 7.10 (t, 1H, ArH), 6.99 (d, 1H, ArH), 6.81 (d, 1H, PyH), 2.50 (s, 3H, CH₃). ^{13}C NMR (126 MHz, DMSO) δ 162.32, 161.87, 160.11, 159.23, 138.12, 133.03, 132.72, 121.85, 121.36, 119.77, 115.61, 112.22, 23.70.

2. 2. 2. 2-(Cyclopropyliminomethyl)-5-fluorophenol (HL²)

4-Fluorosalicylaldehyde (1.40 g, 0.01 mol) and cyclopropylamine (0.57 g, 0.01 mol) were reacted in methanol (50 mL) for 30 min at 20 °C. The solvent was removed by distillation to give yellow product of HL². Analysis Calcd. (%) for C₁₀H₁₀FN₂O: C 67.03, H 5.62, N 7.82. Found (%): C 67.16, H 5.54, N 7.96. IR data (KBr, cm⁻¹): 1627 (CH=N). UV in acetonitrile (λ, ε): 233 nm, 1.51 × 10⁴ L mol⁻¹ cm⁻¹; 265 nm, 8.38 × 10³ L mol⁻¹ cm⁻¹; 346 nm, 5.10 × 10³ L mol⁻¹ cm⁻¹. ^1H NMR (300 MHz, *d*⁶-DMSO): δ 12.15 (s, 1H, OH), 8.67 (s, 1H, CH=N), 7.61 (d, 1H, ArH), 6.87 (d, 1H, ArH), 6.43 (s, 1H, ArH), 1.82 (m, 1H, CH), 0.71 (m, 2H, CH₂), 0.43 (m, 2H, CH₂). ^{13}C NMR (126 MHz, DMSO) δ 167.13, 162.77, 161.10, 132.05, 120.54, 109.23, 103.82, 35.11, 6.77.

2. 2. 3. 5-Bromo-2-[(3-morpholin-4-ylpropylimino)methyl]phenol (HL³)

4-Bromosalicylaldehyde (2.01 g, 0.01 mol) and 3-morpholin-4-ylpropylamine (1.44 g, 0.01 mol) were reacted in methanol (50 mL) for 30 min at 20 °C. The solvent was removed by distillation to give yellow product of HL³. Analysis Calcd. (%) for C₁₄H₁₉BrN₂O₂: C 51.39, H 5.85, N 8.56. Found (%): C 51.31, H 5.77, N 8.71. IR data (KBr, cm⁻¹): 1633 (CH=N). UV in acetonitrile (λ, ε): 228 nm,

1.36 × 10⁴ L mol⁻¹ cm⁻¹; 274 nm, 6.73 × 10³ L mol⁻¹ cm⁻¹; 335 nm, 3.35 × 10³ L mol⁻¹ cm⁻¹. ^1H NMR (300 MHz, *d*⁶-DMSO): δ 11.78 (s, 1H, OH), 8.58 (s, 1H, CH=N), 7.51 (d, 1H, ArH), 7.47 (s, 1H, ArH), 7.11 (d, 1H, ArH), 3.68 (t, 2H, CH₂), 3.60 (q, 4H, CH₂), 2.43 (t, 2H, CH₂), 2.27 (q, 4H, CH₂), 1.72 (m, 2H, CH₂). ^{13}C NMR (126 MHz, DMSO) δ 162.11, 156.35, 133.20, 125.07, 124.31, 120.89, 114.34, 67.18, 62.83, 59.22, 54.71, 29.67.

2. 3. Synthesis of the Complexes

2. 3. 1. [Zn₂I₂(L¹)₂] (1)

Then, a methanol solution (20 mL) of ZnI₂ (0.319 g, 1.0 mmol) was added to the methanol solution of HL¹ (0.212 g, 1.0 mmol). The mixture was stirred for 1 h at 20 °C to give a colorless solution. Colorless block-shaped single crystals suitable for X-ray diffraction were formed by slow evaporation of the solution in air for several days. The yield was 45% (based on HL¹). Analysis Calcd. (%) for C₂₆H₂₂I₂N₄O₂Zn₂: C 38.69, H 2.75, N 6.94, Zn 16.20. Found (%): C 38.82, H 2.63, N 6.85, Zn 16.37. IR data (KBr, cm⁻¹): 1615 (CH=N). UV in acetonitrile (λ, ε): 310 nm, 3.13 × 10³ L mol⁻¹ cm⁻¹; 410 nm, 2.32 × 10³ L mol⁻¹ cm⁻¹. ^1H NMR (300 MHz, *d*⁶-DMSO): δ 8.71 (s, 1H, CH=N), 7.81–7.45 (m, 4H, ArH and PyH), 7.10 (t, 1H, ArH), 6.92 (d, 1H, ArH), 6.82 (d, 1H, PyH), 2.50 (s, 3H, CH₃). ^{13}C NMR (126 MHz, DMSO) δ 163.41, 162.02, 161.05, 159.33, 138.17, 132.92, 132.65, 121.82, 121.71, 120.14, 115.66, 112.31, 23.70.

2. 3. 2. [Zn(HL²)₂(NCS)₂] (2)

A methanol solution (20 mL) of Zn(ClO₄)₂·6H₂O (0.372 g, 1.0 mmol) and ammonium thiocyanate (0.076 g, 1.0 mmol) was added to the methanol solution of HL² (0.179 g, 1.0 mmol). The mixture was stirred for 1 h at 20 °C to give a colorless solution. Colorless block-shaped single crystals suitable for X-ray diffraction were formed by slow evaporation of the solution in air for several days. The yield was 37% (based on HL²). Analysis Calcd. (%) for C₂₂H₂₀F₂N₄O₂S₂Zn: C 48.94, H 3.73, N 10.38, Zn 12.11. Found (%): C 49.13, H 3.82, N 10.28, Zn 12.35. IR data (KBr, cm⁻¹): 2073 (NCS), 1653 (CH=NH). UV in acetonitrile (λ, ε): 270 nm, 3.56 × 10³ L mol⁻¹ cm⁻¹; 305 nm, 1.91 × 10³ L mol⁻¹ cm⁻¹; 350 nm, 8.33 × 10² L mol⁻¹ cm⁻¹; 397 nm, 2.06 × 10² L mol⁻¹ cm⁻¹. ^1H NMR (300 MHz, *d*⁶-DMSO): δ 10.82 (s, 1H, NH), 8.75 (s, 1H, CH=N), 7.61 (d, 1H, ArH), 6.87 (d, 1H, ArH), 6.46 (s, 1H, ArH), 1.83 (m, 1H, CH), 0.71 (m, 2H, CH₂), 0.43 (m, 2H, CH₂). ^{13}C NMR (126 MHz, DMSO) δ 167.35, 162.45, 163.27, 135.86, 132.13, 119.71, 109.43, 104.51, 34.78, 6.77.

2. 3. 3. [ZnIL³] (3)

A methanol solution (20 mL) of ZnI₂ (0.319 g, 1.0 mmol) was added to the methanol solution of HL³ (0.326 g,

1.0 mmol). The mixture was stirred for 1 h at 20 °C to give a colorless solution. Colorless block-shaped single crystals suitable for X-ray diffraction were formed by slow evaporation of the solution in air for several days. The yield was 54% (based on HL³). Analysis Calcd. (%) for C₁₄H₁₈BrIN₂O₂Zn: C 32.43, H 3.50, N 5.40, Zn 12.61. Found (%): C 32.27, H 3.63, N 5.45, Zn 12.82. IR data (KBr, cm⁻¹): 1637 (CH=N). UV in acetonitrile (λ, ε): 225 nm, 3.78 × 10³ L mol⁻¹ cm⁻¹; 242 nm, 3.11 × 10³ L mol⁻¹ cm⁻¹; 278 nm, 1.85 × 10³ L mol⁻¹ cm⁻¹; 357 nm, 9.28 × 10² L mol⁻¹ cm⁻¹. ¹H NMR (300 MHz, d⁶-DMSO): δ 8.67 (s, 1H, CH=N), 7.50 (d, 1H, ArH), 7.45 (s, 1H, ArH), 7.11 (d, 1H, ArH), 3.67 (t, 2H, CH₂), 3.62 (q, 4H, CH₂), 2.37 (t, 2H, CH₂), 2.27 (q, 4H, CH₂), 1.73 (m, 2H, CH₂). ¹³C NMR (126 MHz, DMSO) δ 164.32, 158.11, 132.87, 125.12, 124.26, 121.81, 114.51, 67.25, 63.02, 59.38, 54.66, 29.71.

2. 4. X-Ray Diffraction

Data were collected from selected crystals mounted on glass fibres. The data were collected with MoK_α radiation (0.71073 Å) at 298(2) K with a Bruker SMART 1000 CCD area diffractometer. The data for the complexes were

processed with SAINT⁹ and corrected for absorption using SADABS.¹⁰ Multi-scan absorption corrections were applied with ψ-scans.¹¹ The structures were solved by direct method using SHELXS-97 and refined by full-matrix least-squares techniques on F² using anisotropic displacement parameters.¹² The imino H atom in complex **2** was located from a difference Fourier map and refined with N-H distance of 0.90(1) Å. All other hydrogen atoms were placed at the calculated positions. Idealized H atoms were refined with isotropic displacement parameters set to 1.2 (1.5 for methyl groups) times the equivalent isotropic U values of the parent carbon atoms. The crystallographic data for the complexes are listed Table 1.

Supplementary material has been deposited with the Cambridge Crystallographic Data Centre (nos. 1448092 (**1**), 1975485 (**2**), 1975486 (**3**)); deposit@ccdc.cam.ac.uk or <http://www.ccdc.cam.ac.uk>).

2. 5. Antimicrobial Assay

Qualitative determination of antimicrobial activity was done using the disk diffusion method.¹³ The antibac-

Table 1. Crystallographic data and experimental details for the complexes

	1	2	3
Molecular formula	C ₂₆ H ₂₂ I ₂ N ₄ O ₂ Zn ₂	C ₂₂ H ₂₀ F ₂ N ₄ O ₂ S ₂ Zn	C ₁₄ H ₁₈ BrIN ₂ O ₂ Zn
Formula weight	807.02	539.91	518.48
Crystal size, mm	0.27×0.26×0.26	0.23×0.22×0.21	0.17×0.15×0.15
Radiation (λ, Å)	MoK _α (0.71073)	MoK _α (0.71073)	MoK _α (0.71073)
Crystal system	Triclinic	Monoclinic	Monoclinic
Space group	<i>P</i> -1	<i>P</i> 2/ <i>c</i>	<i>P</i> 2 ₁ / <i>c</i>
Unit cell dimensions:			
<i>a</i> , Å	8.056(2)	10.920(1)	15.065(2)
<i>b</i> , Å	8.659(2)	7.021(1)	9.023(1)
<i>c</i> , Å	11.034(2)	16.122(1)	12.860(1)
α, °	78.264(2)	90	90
β, °	74.640(2)	97.347(1)	105.203(1)
γ, °	69.431(2)	90	90
<i>V</i> , Å ³	689.7(3)	1225.9(3)	1687.0(3)
<i>Z</i>	1	2	4
ρ _{calcd} , g cm ⁻³	1.943	1.463	2.041
<i>F</i> (000)	388	552	1000
<i>T</i> _{min} , <i>T</i> _{max}	0.4109, 0.4222	0.7678, 0.7847	0.4463, 0.4840
Absorption coefficient, mm ⁻¹	4.007	1.213	5.659
θ Range for data collection, °	1.93–25.49	1.88–25.50	1.40–25.50
Reflections collected	4159	6294	33117
Independent reflections (<i>R</i> _{int})	2571 (0.0315)	2287 (0.0495)	3135 (0.0809)
Reflections with <i>I</i> > 2σ(<i>I</i>)	1832	1473	2431
Data/parameters	2571/164	2287/154	3135/190
Restraints	0	1	0
Goodness-of-fit on <i>F</i> ²	1.040	1.024	1.058
Final <i>R</i> indices (<i>I</i> > 2σ(<i>I</i>))	<i>R</i> ₁ = 0.0457 <i>wR</i> ₂ = 0.0878	<i>R</i> ₁ = 0.0688 <i>wR</i> ₂ = 0.1835	<i>R</i> ₁ = 0.0404 <i>wR</i> ₂ = 0.0936
<i>R</i> indices (all data)	<i>R</i> ₁ = 0.0736 <i>wR</i> ₂ = 0.1026	<i>R</i> ₁ = 0.1057 <i>wR</i> ₂ = 0.2073	<i>R</i> ₁ = 0.0605 <i>wR</i> ₂ = 0.1081
Δρ _{max} , Δρ _{min} , e Å ⁻³	1.38, -0.55	1.47, -0.39	0.84, -0.64

terial activity was tested against *B. subtilis*, *E. coli*, *P. fluorescens* and *S. aureus* using MH medium (Mueller–Hinton medium). The MICs (minimum inhibitory concentrations) of the test compounds were determined by a colorimetric method using the dye MTT [3-(4,5-dimethylthiazol-2-yl)-2,5-diphenyltetrazolium bromide]. A stock solution of the synthesized compound ($50 \mu\text{g mL}^{-1}$) in DMSO was prepared and quantities of the test compounds were incorporated in specified quantity of sterilized liquid MH medium. A specified quantity of the medium containing the compound was poured into micro-titration plates. A suspension of the microorganism was prepared to contain approximately 10^5 cfu mL^{-1} and applied to micro-titration plates with serially diluted compounds in DMSO to be tested and incubated at 37°C for 24 h. After the MICs were visually determined on each of the micro-titration plates, $50 \mu\text{L}$ of PBS containing 2 mg of MTT per millilitre was added to each well. Incubation was continued at room temperature for 4–5 h. The content of each well was removed and $100 \mu\text{L}$ of isopropanol containing hydrochloric acid was added to extract the dye. After 12 h of incubation at room temperature, the optical density (OD) was measured with a micro-plate reader at 550 nm.

3. Results and Discussion

3.1. Chemistry

The Schiff bases were readily prepared by the reaction of equimolar quantities of aldehyde and amines in methanol, which were used directly for the preparation of the zinc complexes at ambient temperature. The zinc complexes are stable at room temperature in the solid state and soluble in common organic solvents, such as methanol, ethanol, chloroform, and acetonitrile. The results of the elemental analyses are in accord with the composition suggested for the complexes.

3.2. IR and Electronic Spectra

The IR spectra of the complexes were analyzed and compared with those of their free Schiff bases. The intense absorption bands at 1623 , 1627 and 1633 cm^{-1} in the spectra of the Schiff bases HL¹, HL² and HL³, respectively, can be assigned to the C=N stretching. In the complexes, these bands are shifted to 1615 , 1653 and 1637 cm^{-1} upon complexation with the zinc atoms, which can be attributed to the coordination of the imine nitrogen to the metal centre.¹⁴ The absorption of this band for complex 2 is located at higher wavelength than complexes 2 and 3, which is due to the protonation of the imino group. The typical absorption at 2073 cm^{-1} in the spectrum of complex 2 is assigned to the vibration of the NCS ligand.¹⁵

UV–Vis spectra of the free Schiff bases and the complexes were recorded in HPLC grade acetonitrile solution. The spectra of the Schiff bases exhibit bands at 220–280

nm and 330–360 nm attributed to $\pi \rightarrow \pi^*$ and $n \rightarrow \pi^*$ transitions. In the spectra of the complexes the charge transfer bands at 220–280 nm remain intact, in agreement with the $\pi \rightarrow \pi^*$ transitions of the Schiff base ligands. The remaining bands at 350–410 nm in the spectra of the complexes are assigned to the metal to ligand charge transfer (MLCT) transition.¹⁶

3.3. NMR Spectra

The ¹H NMR spectra of the Schiff bases exhibit OH (phenolic) proton resonances at 11.78–12.15 ppm, imine proton resonances at 8.58–8.67 ppm and aromatic proton resonances in the range 6.43–7.68 ppm, respectively. On coordination, the signal due to OH proton disappears, indicating deprotonation of the phenolic OH and subsequent coordination of the phenoxide oxygen to the metal atoms. Involvement of the imine nitrogen in coordination has shifted the resonance signal of the imine proton by 0.7–0.9 ppm. The peaks observed in ¹³C NMR spectra of the Schiff bases and the complexes are in expected range and values are given in experimental section. The carbonyl C and imine C atoms in the complexes have shifted compared to their ligands, confirming the coordination through carbonyl O and imine N atoms.¹⁷

3.4. Crystal Structure Description of the Complexes

Complex 1 is a phenolato-bridged dinuclear zinc(II) compound (Figure 1), with Zn...Zn separation of 3.096(2) Å. The crystal of the complex possesses a crystallographic inversion symmetry, with the inversion center located at the middle of the two zinc atoms. The Zn atom in the complex is coordinated by one pyridine N and two phenolate O atoms from two Schiff base ligands, and one I atom, generating tetrahedral geometry. The Schiff base acts as a bidentate ligand, and forms a six-membered chelate ring with the metal center through the phenolate O and imine N. The bond distances subtended at the metal atoms are

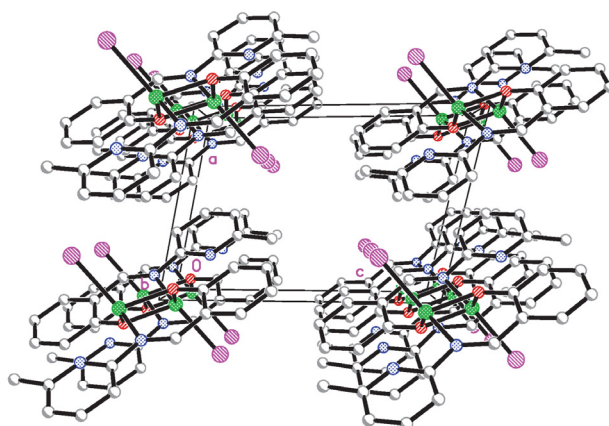


Figure 2. Molecular packing structure of complex 1.

comparable to those observed in similar zinc(II) complexes with Schiff bases.¹⁸

In the crystal structure of the complex, molecules are stacked *via* $\pi\cdots\pi$ interactions (Table 3) along the *b* axis (Figure 2).

Complex 2 is a thiocyanate-coordinated mononuclear zinc(II) compound (Figure 3). The Zn atom in the complex is coordinated by two phenolate O atoms from two zwitterionic Schiff base ligands, and two thiocyanate N atoms, generating tetrahedral geometry. The Schiff base

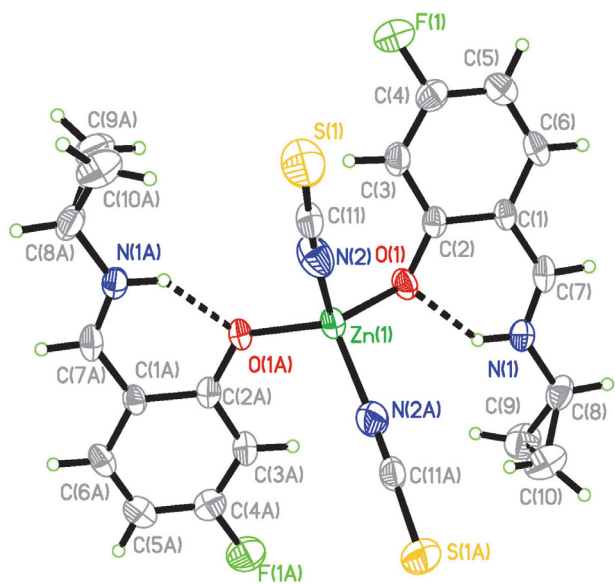


Figure 3. Molecular structure of complex 2. Atoms labeled with the suffix A are at the symmetry position $-x, y, 1/2 - z$.

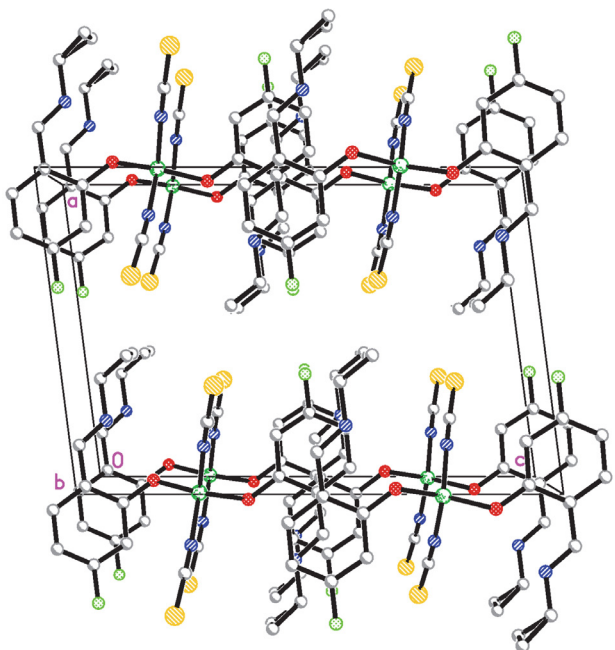


Figure 4. Molecular packing structure of complex 2.

acts as a monodentate ligand, with the phenol H atom transferred to the imino N group. The bond distances subtended at the metal atoms are comparable to those observed in similar zinc(II) complexes with Schiff bases and thiocyanate ligands.¹⁹

In the crystal structure of the complex, molecules are stacked *via* $\pi\cdots\pi$ interactions (Table 3) including the pyridine ring N(2)-C(8)-C(12)-C(11)-C(10)-C(9) and the chelate ring Zn(1)-N(1)-C(8)-N(2), along the *b* axis (Figure 4).

Complex 3 is an iodide-coordinated mononuclear zinc(II) compound (Figure 5). The Zn atom in the complex is coordinated by one phenolate O, one imino N, and one morpholine N atoms of the Schiff base ligand, and one I atom, generating tetrahedral geometry. The Schiff base acts as a tridentate ligand, with the morpholine ring adopts chair configuration. The bond distances subtended at the metal atoms are comparable to those observed in similar zinc(II) complexes with Schiff bases and thiocyanate ligands.²⁰

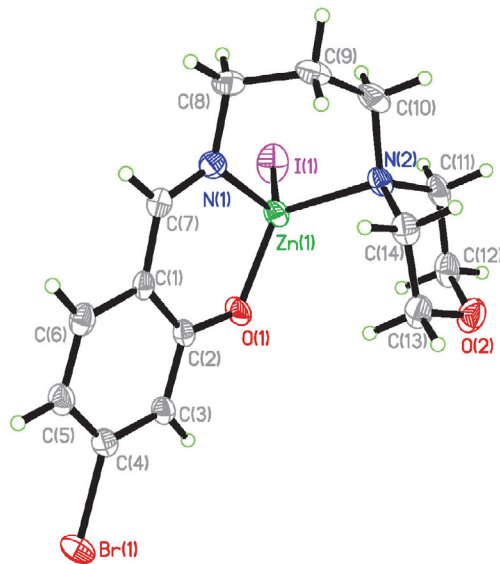


Figure 5. Molecular structure of complex 3.

In the crystal structure of the complex, molecules are stacked *via* $\pi\cdots\pi$ interactions (Table 3) including the phenyl ring C(1)-C(2)-C(3)-C(4)-C(5)-C(6) and the chelate ring Zn(1)-O(1)-C(2)-C(1)-C(7)-N(1), along the *b* axis (Figure 6).

3. 5. Antimicrobial Activity

The results of the antimicrobial activity are summarized in Table 4. A comparative study of minimum inhibitory concentration (MIC) values of the Schiff base and the zinc complex indicated that the complex has more effective activity against *Staphylococcus aureus*, *Escherichia coli*, and *Candida albicans* than the free Schiff base. Generally,

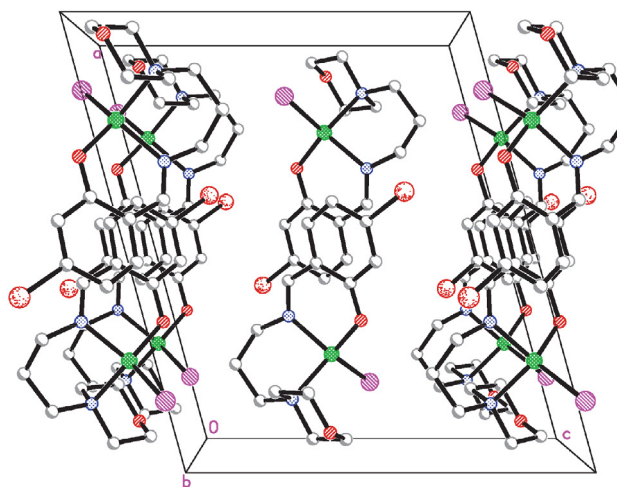


Figure 6. Molecular packing structure of complex 3.

this is caused by the greater lipophilic nature of the complex than the ligand. Such increased activity of the metal chelates can be explained on the basis of chelating theory.²¹ On chelating, the polarity of the metal atoms will be reduced to a greater extent due to the overlap of the ligand orbital and partial sharing of positive charge of the metal atoms with donor atoms. Further, it increases the delocalization of π -electrons over the whole chelate ring and enhances the lipophilicity of the complex. This increased lipophilicity enhances the penetration of the complex into lipid membrane and blocks the metal binding sites on enzymes of micro-organisms.

The complexes have stronger activities against *Staphylococcus aureus*, *Escherichia coli*, and *Candida albicans* than the free Schiff bases. For *Staphylococcus aureus* and *Escherichia coli*, the activities of the complexes are less than the control drug Tetracycline. But for *Candida albi-*

Table 2. Selected bond distances (Å) and angles (°) for the complexes

1			
Zn(1)–O(1) ^{#1}	1.990(5)	Zn(1)–O(1)	2.080(4)
Zn(1)–N(1)	2.014(5)	Zn(1)–I(1)	2.541(1)
O(1)–Zn(1)–N(1) ^{#1}	122.3(2)	O(1)–Zn(1)–O(1) ^{#1}	81.0(2)
O(1)–Zn(1)–N(1)	88.1(2)	O(1)–Zn(1)–I(1) ^{#1}	113.3(1)
N(1)–Zn(1)–I(1)	122.9(2)	O(1)–Zn(1)–I(1)	113.1(1)
2			
Zn(1)–O(1)	1.929(4)	Zn(1)–N(2)	1.958(6)
O(1)–Zn(1)–O(1) ^{#2}	117.1(2)	O(1)–Zn(1)–N(2)	109.8(2)
O(1)–Zn(1)–N(2) ^{#2}	103.8(2)	N(2)–Zn(1)–N(2) ^{#2}	112.7(4)
3			
Zn(1)–I(1)	2.5319(8)	Zn(1)–O(1)	1.905(4)
Zn(1)–N(1)	1.989(5)	Zn(1)–N(2)	2.111(4)
O(1)–Zn(1)–N(1)	96.47(18)	O(1)–Zn(1)–N(2)	120.94(19)
N(1)–Zn(1)–N(2)	94.06(19)	O(1)–Zn(1)–I(1)	116.24(13)
N(1)–Zn(1)–I(1)	119.21(14)	N(2)–Zn(1)–I(1)	107.99(12)

Symmetry codes: ^{#1} – $x, 1 - y, 2 - z$; ^{#2} – $x, 1 - y, 2 - z$.

Table 3. Parameters between the planes for the complexes

Cg	Distance between ring centroids (Å)	Dihedral angle (°)	Perpendicular distance of Cg(I) on Cg(J) (Å)	Beta angle (°)	Gamma angle (°)	Perpendicular distance of Cg(J) on Cg(I) (Å)
1						
Cg(1)–Cg(2) ^{#1}	3.879	4.877	3.4456	32.19	27.34	3.2826
Cg(2)–Cg(2) ^{#1}	3.657	0	3.3852	22.24	22.24	3.3852
Cg(2)–Cg(3) ^{#2}	3.664	2.391	–3.4737	18.96	18.56	–3.4655
2						
Cg(4)–Cg(4) ^{#3}	4.152	0	–3.428	34.36	34.36	–3.428
3						
Cg(5)–Cg(6) ^{#4}	4.143	2.088	–3.295	37.02	37.33	–3.308
Cg(6)–Cg(6) ^{#5}	4.260	0	3.654	30.91	30.91	3.654

1: Cg(1), Cg(2) and Cg(3) are the centroids of Zn(1)–N(1)–C(8)–N(2), N(2)–C(8)–C(12)–C(11)–C(10)–C(9) and C(1)–C(2)–C(3)–C(4)–C(5)–C(6), respectively. 2: Cg(4) is the centroid of C(1)–C(2)–C(3)–C(4)–C(5)–C(6). 3: Cg(5) and Cg(6) are the centroids of Zn(1)–O(1)–C(2)–C(1)–C(7)–N(1) and C(1)–C(2)–C(3)–C(4)–C(5)–C(6), respectively. Symmetry codes: ^{#1}: $1 - x, 1 - y, -z$; ^{#2}: $2 - x, 1 - y, -z$; ^{#3}: $-x, 1 - y, -z$; ^{#4}: $1 - x, 1 - y, 1 - z$; ^{#5}: $1 - x, 2 - y, 1 - z$.

cans, the complexes have stronger activities than Tetracycline. Complex **2** has the most activity against *Staphylococcus aureus* with MIC value of 2 µg/mL. The three zinc complexes have higher activities against *Staphylococcus aureus* and lower activities against *Escherichia coli* and *Candida albicans* than the zinc(II) and manganese(II) complexes with the ligand *N*'-(1-(pyridin-2-yl)ethylidene)isonicotinohydrazide.²² Further work needs to be carried out to investigate the structure-activity relationship.

Table 4. MIC values (µg/mL) for the antimicrobial activities of the tested compounds

Compound	<i>Staphylococcus aureus</i>	<i>Escherichia coli</i>	<i>Candida albicans</i>
HL ¹	128	256	> 1024
HL ²	128	128	> 1024
HL ³	64	256	> 1024
1	4	16	128
2	2	32	256
3	4	32	256
Tetracycline	0.25	2.0	> 1024

4. Conclusions

In summary, three new zinc(II) complexes with halide and pseudohalide ligands derived from Schiff bases have been prepared and characterized. The structures of the complexes are confirmed by single crystal X-ray crystallographic determination. The Zn atoms in the complexes are in tetrahedral coordination. The complexes have better activities on the bacteria *Staphylococcus aureus* and *Escherichia coli* than the control drug Tetracycline. Moreover, the complexes have stronger activities against *Candida albicans* than Tetracycline. Interestingly, complex **2** has the most activity against *Staphylococcus aureus* with MIC value of 2 µg/mL.

5. Acknowledgments

This research was supported by the National Sciences Foundation of China (nos. 20676057 and 20877036) and Top-class foundation of Pingdingshan University (no. 2008010).

6. References

- L. N. Obasi, J. C. Ezeorah, V. Ossai, A. Jude, U. S. Oruma, A. Ibezim, M. Lutter, L. Rhyman, K. Jurkschat, N. Dege, P. Ramasami, *J. Mol. Struct.* **2019**, *1188*, 69–75. DOI:10.1016/j.molstruc.2019.03.081
- (a) S. K. Bharti, G. Nath, R. Tilak, S. K. Singh, *Eur. J. Med. Chem.* **2010**, *45*, 651–660; DOI:10.1016/j.ejmech.2009.11.008
(b) M. Ceruso, F. Carta, S. M. Osman, Z. Allothman, S. M. Monti, C. T. Supuran, *Bioorg. Med. Chem.* **2015**, *23*, 4181–4187; DOI:10.1016/j.bmc.2015.06.050
(c) W. L. Wang, D. Agustin, R. Poll, *Mol. Catal.* **2017**, *443*, 52–59; DOI:10.1016/j.mcat.2017.09.033
(d) M. Hanif, M. Hassan, M. Rafiq, Q. Abbas, A. Ishaq, S. Shahzadi, S.-Y. Seo, M. Saleem, *Pharm. Chem. J.* **2018**, *52*, 424–437; DOI:10.1007/s11094-018-1835-0
(e) P. Mishra, P. N. Gupta, K. Ashok, R. Shukla, R. C. Srimal, *Indian J. Physiol. Pharm.* **1995**, *39*, 169–172.
- (a) K. Venkateswarlu, N. Ganji, S. Daravath, K. Kanneboina, K. Rangan, Shivaraj, *Polyhedron* **2019**, *171*, 86–97; DOI:10.1016/j.poly.2019.06.048
(b) R. A. Ammar, A. N. M. A. Alaghaz, M. E. Zayed, L. A. Al-Bedair, *J. Mol. Struct.* **2017**, *1141*, 368–381; DOI:10.1016/j.molstruc.2017.03.080
(c) N. R. Palepu, S. L. Nongbri, J. R. Premkumar, A. K. Verma, K. Bhattacharjee, S. R. Joshi, S. Forbes, Y. Mozharivskiy, R. Thounaojam, K. Aguan, M. R. Kollipara, *J. Biol. Inorg. Chem.* **2015**, *20*, 619–638; DOI:10.1007/s00775-015-1249-3
(d) M. Aidi, H. Keypour, A. Shooshtari, M. Mahmoud-abadi, M. Bayat, Z. Ahmadvand, R. Karamian, M. Asadbegy, S. Tavatli, R. W. Gable, *Polyhedron* **2019**, *167*, 93–102. DOI:10.1016/j.poly.2019.02.030
- (a) C. X. Yuan, L. P. Lu, X. L. Gao, Y. B. Wu, M. L. Guo, Y. Li, X. Q. Fu, M. L. Zhu, *J. Bio. Inorg. Chem.* **2009**, *14*, 841–851; DOI:10.1007/s00775-009-0496-6
(b) P. A. Khalf-Alla, S. S. Hassan, M. M. Shoukry, *Inorg. Chim. Acta* **2019**, *492*, 192–197; DOI:10.1016/j.ica.2019.04.035
(c) S. Daravath, A. Rambabu, N. Vamsikrishna, N. Ganji, S. Raj, *J. Coord. Chem.* **2019**, *72*, 1973–1993; DOI:10.1080/00958972.2019.1634263
(d) M. S. S. Adam, L. H. Abdel-Rahman, A. M. Abu-Dief, N. A. Hashem, *Inorg. Nano-Met. Chem.* **2019**, *50*, 136–150; DOI:10.1080/24701556.2019.1672735
(e) M. Sonmez, M. Celebi, I. Berber, *Eur. J. Med. Chem.* **2010**, *45*, 1935–1940; DOI:10.1016/j.ejmech.2010.01.035
(f) L. W. Xue, G. Q. Zhao, Y. J. Han, Y. X. Feng, *Russ. J. Coord. Chem.* **2011**, *37*, 262–269; DOI:10.1134/S1070328411030110
(g) L. W. Xue, Y. J. Han, G. Q. Zhao, Y. X. Feng, *Russ. J. Coord. Chem.* **2012**, *38*, 24–28. DOI:10.1134/S1070328411120104
- (a) Q.-M. Hasi, Y. Fan, X.-X. Feng, X.-Q. Yao, J.-C. Liu, *Transition Met. Chem.* **2016**, *41*, 685–692; DOI:10.1007/s11243-016-0069-9
(b) P. A. Khalf-Alla, S. S. Hassan, M. M. Shoukry, *Inorg. Chim. Acta* **2019**, *492*, 192–197; DOI:10.1016/j.ica.2019.04.035
(c) S. Daravath, A. Rambabu, N. Vamsikrishna, N. Ganji, S. Raj, *J. Coord. Chem.* **2019**, *72*, 1973–1993; DOI:10.1080/00958972.2019.1634263
(d) M. S. S. Adam, L. H. Abdel-Rahman, A. M. Abu-Dief, N. A. Hashem, *Inorg. Nano-Met. Chem.* **2019**, *50*, 136–150. DOI:10.1080/24701556.2019.1672735
- M. Zhang, D.-M. Xian, H.-H. Li, J.-C. Zhang, Z.-L. You, *Aust. J. Chem.* **2012**, *65*, 343–350. DOI:10.1071/CH11424

7. (a) L.-W. Xue, H.-J. Zhang, P.-P. Wang, *Acta Chim. Slov.* **2019**, *66*, 190–195;
 (b) G.-X. He, L.-W. Xue, Q.-L. Peng, P.-P. Wang, H.-J. Zhang, *Acta Chim. Slov.* **2019**, *66*, 570–575;
DOI:10.17344/acsi.2018.4868
 (c) L.-W. Xue, Y.-J. Han, X.-Q. Luo, *Acta Chim. Slov.* **2019**, *66*, 622–628. **DOI**:10.17344/acsi.2019.5039
8. (a) A. Castineiras, J. A. Castro, M. L. Duran, J. A. Garcia-Vazquez, A. Macias, J. Romero, A. Sousa, *Polyhedron* **1989**, *8*, 2543–2549; **DOI**:10.1016/S0277-5387(00)81154-7
 (b) L. Xu, Y. V. Mironov, X. Qi, S.-J. Kim, *J. Struct. Chem.* **2006**, *47*, 998–1001. **DOI**:10.1007/s10947-006-0418-1
9. Bruker, SMART and SAINT, *Area Detector Control and Integration Software*, Madison (WI, USA): Bruker Analytical X-ray Instruments Inc., 1997.
10. G. M. Sheldrick, SADABS, *Program for Empirical Absorption Correction of Area Detector Data*, Göttingen (Germany): Univ. of Göttingen, 1997.
11. A. C. T. North, D. C. Phillips, F. S. Mathews, *Acta Crystallogr. A* **1968**, *24*, 351–359. **DOI**:10.1107/S0567739468000707
12. G. M. Sheldrick, SHELXL-97, *Program for the Refinement of Crystal Structures*, Göttingen (Germany): Univ. of Göttingen, 1997.
13. (a) A. Barry, *Procedures and Theoretical Considerations for Testing Antimicrobial Agents in Agar Media*, In: *Antibiotics in Laboratory Medicine*, Lorian, V., Ed., Baltimore: Williams and Wilkins, 1991;
 (b) T. Rosu, M. Negoiu, S. Pasculescu, E. Pahontu, D. Poirier, A. Gulea, *Eur. J. Med. Chem.* **2010**, *45*, 774–781.
DOI:10.1016/j.ejmech.2009.10.034
14. A. Ray, D. Sadhukhan, G. M. Rosair, C. J. Gomez-Garcia, S. Mitra, *Polyhedron* **2009**, *28*, 3542–3550.
DOI:10.1016/j.poly.2009.07.017
15. S. B. asak, S. Sen, S. Banerjee, S. Mitra, G. Rosair, M. T. G. Rodriguez, *Polyhedron* **2007**, *26*, 5104–5112.
DOI:10.1016/j.poly.2007.07.025
16. M. Enamullah, M. A. Quddus, M. A. Halim, M. K. Islam, V. Vasylyeva, C. Janiak, *Inorg. Chim. Acta* **2015**, 103–111.
DOI:10.1016/j.ica.2014.11.020
17. D. S. Badiger, R. S. Hunoor, B. R. Patil, R. S. Vadavi, C. V. Mangannavar, I. S. Muchchandi, Y. P. Patil, M. Nethaji, K. B. Gudasi, *Inorg. Chim. Acta* **2012**, 197–203.
DOI:10.1016/j.ica.2011.11.063
18. (a) F.-W. Wang, Y.-J. Wei, Q.-Y. Zhu, *Chin. J. Struct. Chem.* **2007**, *26*, 1327–1331;
 (b) Z.-L. You, X. Han, J. Wang, J.-Y. Chi, *Chin. J. Struct. Chem.* **2006**, *25*, 1043–1046;
 (c) T. Chattopadhyay, M. Mukherjee, K. S. Banu, A. Banerjee, E. Suresh, E. Zangrando, D. Das, *J. Coord. Chem.* **2009**, *62*, 967–979; **DOI**:10.1080/00958970802385837
 (d) A. Guha, T. Chattopadhyay, N. D. Paul, M. Mukherjee, S. Goswami, T. K. Mondal, E. Zangrando, D. Das, *Inorg. Chem.* **2012**, *51*, 8750–8759; **DOI**:10.1021/ic300400v
 (e) J. Qin, Y. Sun, Z. N. Xia, Y. Zhang X. L. Zhao, Z. L. You, H. L. Zhu, *Russ. J. Coord. Chem.* **2016**, *42*, 330–337.
DOI:10.1134/S1070328416050055
19. (a) N. Wang, L. Chen, L. Yang, Y. Wan, *Synth. React. Inorg. Met.-Org. Nano-Met. Chem.* **2014**, *44*, 315–319;
DOI:10.1080/15533174.2013.770763
 (b) D.-H. Shi, Z.-L. Cao, W.-W. Liu, R.-B. Xu, L.-L. Gao, Q. Zhang, *Synth. React. Inorg. Met.-Org. Nano-Met. Chem.* **2012**, *42*, 864–867. **DOI**:10.1080/15533174.2011.618483
20. (a) J.-N. Li, *Synth. React. Inorg. Met.-Org. Nano-Met. Chem.* **2013**, *43*, 832–837;
 (b) S. S. Qian, X. S. Cheng, J. Q. Ren, Z. L. You, H. L. Zhu, *Russ. J. Coord. Chem.* **2013**, *39*, 836–843.
DOI:10.1134/S1070328413110080
21. J. W. Searl, R. C. Smith, S. Wyard, *J. Proc. Phys. Soc.* **1961**, *78*, 1174–1178. **DOI**:10.1088/0370-1328/78/6/311
22. L.-W. Xue, H.-J. Zhang, P.-P. Wang, *Acta Chim. Slov.* **2019**, *66*, 190–195.

Povzetek

Trije novi cinkovi (II) kompleksi, $[Zn_2I_2(L^1)_2]$ (**1**), $[Zn(HL^2)_2(NCS)_2]$ (**2**) in $[ZnIL^3]$ (**3**), kjer je L^1 anionska oblika 2-[(6-metilpiridin-2-ilimino)metil]fenola (HL^1), HL^2 je zwitterionska oblika 2-(ciklopropiliminometil)-5-fluorofenola (HL^2) in L^3 je anionska oblika 5-bromo-2-[(3-morfolin-4-ilpropilimino)metil]fenol (HL^3), so bili pripravljene in karakterizirani z elementno analizo, IR, UV in NMR spektroskopijo ter rentgensko difrakcijo na monokristalih. Kompleks **1** je dvojedrni cinkov kompleks, kompleksa **2** in **3** pa sta enojedrni cinkova kompleksa. Atomi Zn v kompleksih so v tetraedrski koordinaciji. Preučevana je bila tudi protimikrobna aktivnost kompleksov proti *Staphylococcus aureus*, *Escherichia coli* in *Candida albicans*.



Except when otherwise noted, articles in this journal are published under the terms and conditions of the Creative Commons Attribution 4.0 International License